Duality between two generalized Aubry-André models with exact mobility edges

Yucheng Wang [1,2,3,*] Xu Xia [4,†] Yongjian Wang [5,6,‡] Zuohuan Zheng,[5,6,7] and Xiong-Jun Liu [2,3,8,1]

[1]*Shenzhen Institute for Quantum Science and Engineering, Southern University of Science and Technology, Shenzhen 518055, China*
[2]*International Center for Quantum Materials, School of Physics, Peking University, Beijing 100871, China*
[3]*Collaborative Innovation Center of Quantum Matter, Beijing 100871, China*
[4]*Chern Institute of Mathematics and LPMC, Nankai University, Tianjin 300071, China*
[5]*Academy of Mathematics and Systems Science, Chinese Academy of Sciences, Beijing 100190, China*
[6]*University of Chinese Academy of Sciences, Beijing 100049, China*
[7]*College of Mathematics and Statistics, Hainan Normal University, Haikou, Hainan 571158, China*
[8]*CAS Center for Excellence in Topological Quantum Computation, University of Chinese Academy of Sciences, Beijing 100190, China*

(Received 22 December 2020; accepted 10 May 2021; published 18 May 2021)

A mobility edge (ME) in energy separating extended from localized states is a central concept in understanding various fundamental phenomena, such as the metal-insulator transition in disordered systems. In one-dimensional quasiperiodic systems, there exist a few models with exact MEs, and these models are beneficial to provide exact understanding of ME physics. Here we investigate two widely studied models including exact MEs, one with an exponential hopping and one with a special form of incommensurate on-site potential. We analytically prove that the two models are mutually dual and further give the numerical verification by calculating the inverse participation ratio and Husimi function. Our result may provide insight into realizing and observing exact MEs in both theory and experiment.

DOI: 10.1103/PhysRevB.103.174205

I. INTRODUCTION

Anderson localization (AL) [1], a fundamental quantum phenomenon in nature, reveals that the single-particle states can become localized due to disorder effect. The quantum phase transition from the extended (metal) phase to the localized (insulator) phase can occur by increasing the disorder strength in three-dimensional (3D) systems. Near the transition point, the mobility edges (MEs) can occur and separate the extended and localized states [2,3]. ME lie at the heart in understanding various fundamental phenomena, such as the metal-insulator transition induced by varying disorder strength or particle number density. Moreover, a system with ME has strong thermoelectric response [4–6] and can be applied to thermoelectric devices. MEs exist widely in 3D systems with random disorder, but for one and two dimensions, the scaling theory [7] shows that all states are localized for arbitrarily small disorder strengths, so no MEs exist.

Unlike random disorder, the quasiperiodic potential can induce the extended-AL transition at a finite strength of the potential even in the one-dimensional (1D) systems, which bring about rich interesting physics, e.g., the existence of MEs even in 1D systems [8–12] and nonergodic critical phases [13–15]. The most celebrated example with 1D quasiperiodic potential is the Aubry-André (AA) model [16], described by $t(\psi_{j+1}+\psi_{j-1})+V\cos(2\pi\beta j+\delta)\psi_j=E\psi_j$, where ψ_j, t, V, and δ denote the wave-function amplitude at site j, the nearest-neighbor hopping strength, the strength of the quasiperiodic potential, and the phase parameter, respectively, and β is an irrational number. The model exhibits a self-duality for the transformation between real and momentum spaces at $V=2t$, leading to the extended-localization transition with all the eigenstates of the model being extended (localized) for $V<2t$ ($V>2t$). Thus, no ME exists for the AA model. This model has been realized in ultracold atomic gases trapped in incommensurate optical lattices, and the localization transition has been observed [17]. The existence of the many-body localization phase in the AA model in the presence of weak interactions has also been well established in both theory [18–20] and experiment [21,22].

By introducing the exponential [8] or power-law [23] hopping term, or breaking the self-duality of the AA model [9,10,24–29], one can obtain the MEs in the system. However, very few of them can provide the accurate expression of MEs [8–10,24], and undoubtedly, these models with exact MEs are beneficial to provide exact understanding of the ME physics for both the noninteracting and interacting systems. In this paper, we will focus on the two most commonly used models with exact MEs and find their relation. One is [8]

$$E_1 a_n=\sum_{n'\neq n} t_1 e^{-p|n-n'|}a_{n'}+V\cos(2\pi\beta n+\delta)a_n, \quad (1)$$

where $p>0$, $t_1e^{-p|n-n'|}$ is the hopping rate between sites n and n' and V is the strength of the quasiperiodic potential. The first term on the right-hand side represents an exponential hopping, which is obviously different from the AA model,

*wangyc3@sustech.edu.cn
†xiaxu14@mails.ucas.ac.cn
‡wangyongjian@amss.ac.cn

but this model will reduce to the AA model in the $p \to \infty$ limit. J. Biddle and Das Sarma first analytically predicted and numerically verified the exact expression of ME [8], which is

$$E_{1c} = V\ \cosh(p) - t_1. \tag{2}$$

The other widely studied model with exact MEs we considered is [9]

$$E_2 b_n = t_2(b_{n-1} + b_{n+1}) + 2\lambda \frac{\cos(2\pi\beta n + \delta)}{1 - \alpha\ \cos(2\pi\beta n + \delta)} b_n, \tag{3}$$

where t_2 represents the hopping strength between neighboring sites, λ, and α [$\alpha \in (-1, 1)$] represent the on-site modulation strength and the deformation parameter, respectively, and when $\alpha = 0$, this model reduces to the AA model. The known exact expression of the ME is [9]

$$E_{2c} = 2\,\mathrm{sgn}(\lambda)(|t_2| - |\lambda|)/\alpha. \tag{4}$$

Analytical and numerical results show that the ME expressions (2) and (4) are independent of the systems boundary conditions, sizes, and the specific value of the parameters δ and β [8,9], which can also be seen from the following calculation of the localization length. Thus, without loss of generality, we take $\delta = 0$, $\beta = (\sqrt{5} - 1)/2$, and open boundary conditions (OBC) in the following numerical calculations. For convenience, we call the above-mentioned first (second) model Model I (II). The two models have widely been used to study the ME physics, e.g., the dynamical behavior of a system with MEs [30], fate of MEs in the presence of interactions [31–34], or non-Hermitian term [35–37].

In recent years, MEs have been observed in disordered systems [38–40] and quasiperiodic systems [41–44] in experiments based on ultracold atoms. In particular, the recent work [44] has accurately realized the Model II (3) by using synthetic lattices of laser-coupled atomic momentum modes, and accurately detected the location of MEs in the absence and presence of interactions.

This paper is motivated by two nontrivial questions raised here. First, is there any nontrivial relation between the above two models even if they seem to be quite different, and whether the Model I can be accurately realized in experiment? Second, can the localization lengths of the states in two models can be exactly computed, which clearly necessitates to go beyond the dual transformation applied to determine the ME in the previous studies? Answering these questions is important to unveil the fundamental properties of the two important models. In this paper, we prove that the above two generalized AA models [Eqs. (1) and (3)] have the mutually dual relation, and further provide exact study of the localization properties of the states. With the dual relation proved in this paper, the recent experimental work [44] that realized Model II (3) in momentum space could be regarded to have also effectively realized Model I in real space.

II. ANALYTICAL AND NUMERICAL RESULTS

A. Analytical derivation for dual relations

We first analytically establish the duality between Model I and Model II. We start from Model I (1) and introduce the transformation,

$$a_j = \frac{1}{\sqrt{L}} \sum_m b_m e^{-i2\pi m\beta j}, \tag{5}$$

where L is the system size, and

$$b_m = \frac{1}{\sqrt{L}} \sum_j a_j e^{i2\pi m\beta j}. \tag{6}$$

By using the transformation (5), Eq. (1) becomes

$$E_1 \frac{1}{\sqrt{L}} \sum_m b_m e^{-i2\pi m\beta n} = \sum_{n' \neq n} t_1 e^{-p|n-n'|} \frac{1}{\sqrt{L}} \sum_m b_m e^{-i2\pi m\beta n'} + V\ \cos(2\pi\beta n) \frac{1}{\sqrt{L}} \sum_m b_m e^{-i2\pi m\beta n}. \tag{7}$$

Here we have set $\delta = 0$. Then, we rewrite the first term on the right side of the equation $\sum_{n' \neq n} t_1 e^{-p|n-n'|} \frac{1}{\sqrt{L}} \sum_m b_m e^{-i2\pi m\beta n'}$ as $\frac{1}{\sqrt{L}} \sum_m b_m e^{-i2\pi m\beta n} \sum_{n' \neq n} t_1 e^{-p|n-n'|} e^{-i2\pi m\beta(n'-n)}$, where $\sum_{n' \neq n} t_1 e^{-p|n-n'|} e^{-i2\pi m\beta(n'-n)}$ is the summation of a geometric sequence, and one can obtain that it equals $\frac{2t_1[-e^{-2p} + e^{-p}\cos(2\pi m\beta)]}{1 + e^{-2p} - 2e^{-p}\cos(2\pi m\beta)}$. Then, Eq. (7) can be written as

$$\begin{aligned} &E_1 \frac{1}{\sqrt{L}} \sum_m b_m e^{-i2\pi m\beta n} \\ &= \frac{1}{\sqrt{L}} \sum_m b_m e^{-i2\pi m\beta n} \frac{2t_1[-e^{-2p} + e^{-p}\cos(2\pi m\beta)]}{1 + e^{-2p} - 2e^{-p}\cos(2\pi m\beta)} \\ &\quad + \frac{V}{2} \frac{1}{\sqrt{L}} \sum_m (b_{m-1} + b_{m+1}) e^{-i2\pi m\beta n}. \end{aligned}$$

Utilizing the above formula, one can directly obtain

$$\begin{aligned} E_1 b_m = &\frac{2t_1[-e^{-2p} + e^{-p}\cos(2\pi m\beta)]}{1 + e^{-2p} - 2e^{-p}\cos(2\pi m\beta)} b_m \\ &+ \frac{V}{2}(b_{m-1} + b_{m+1}). \end{aligned} \tag{8}$$

Let

$$t_2 = \frac{V}{2}, \quad \alpha = \frac{2e^{-p}}{1 + e^{-2p}}, \tag{9a}$$

$$E_2 = E_1 + \frac{2t_1 e^{-2p}}{1 + e^{-2p}}, \quad \lambda = \frac{t_1(-e^{-3p} + e^{-p})}{(1 + e^{-2p})^2}, \tag{9b}$$

then, Eq. (8) is equivalent to Eq. (3). Therefore, Model I [Eq. (1)] and Model II [Eq. (3)] are mutually dual, and their relationship is established by Eqs. (9a) and (9b). A recent experimental work [44] has realized Model II (3) in momentum space and accurately detected the location of MEs, but Model I has not been realized. By using Eqs. (9a) and (9b), the experimental work [44] could be regarded to have also effectively realized Model I in real space and detected the location of MEs. In the following subsection, we discuss an application of the dual relationship in theory.

B. Localization lengths and mobility edges

We have analytically proven that the two models (Model I and Model II) are mutually dual. Actually, we also built a bridge between the models with the exponential hopping and the nearest-neighbor hopping but with a special potential. Typically, a model with the exponential hopping is not easy to solve, but a model with the nearest-neighbor hopping can be written as a tridiagonal matrix, whose ME expression can generally be obtained by using a self-consistent theory [45] or by calculating the localization length numerically by using the recursive methods [46] and analytically by using Avilas global theory [47]. The global theory can even analytically give all states' extended and localized properties, including the localization lengths of localized states. Thus, we can investigate the model with exponential hopping by studying its dual model and their dual relationship. As an example, we will obtain the ME expressions of the two models by using the Avila's global theory [10,47,48] and the dual relationship Eqs. (9a) and (9b). We note that the ME expressions have been obtained in previous work [8,9], and we here calculate them with the aim of displaying an application of the dual relationship in dealing with the model with an exponential hopping. In this process, besides the ME expressions, we also obtain the localization length expression of Model II, which will help us better understand this model.

We first represent Model II [Eq. (3)] in the transfer matrix form

$$\begin{pmatrix} b_{n+1} \\ b_n \end{pmatrix} = T^n \begin{pmatrix} b_n \\ b_{n-1} \end{pmatrix},$$

where the transfer matrix T^n is given by

$$T^n = \begin{pmatrix} \frac{E_2}{t_2} - \frac{2\lambda}{t_2}\frac{\cos(2\pi\beta n+\delta)}{1-\alpha\cos(2\pi\beta n+\delta)} & -1 \\ 1 & 0 \end{pmatrix}. \tag{10}$$

Using the transfer matrix, one can define and compute the Lyapunov exponent (LE),

$$\gamma(E) = \lim_{n\to\infty} \frac{1}{2\pi L} \int \ln \|T_L(\delta)\| d\delta,$$

where $T_L = \prod_{n=1}^{L} T^n$ and $\|T_L\|$ denotes the norm of the matrix T_L. The LE can be exactly obtained by using Avila's global theory [47,48], and the details for the calculation are put in the Appendix B. By the LE, we can obtain the localization length ξ, which is the reciprocal of the LE, i.e.,

$$\xi(E) = \frac{1}{\gamma(E)} = \frac{1}{\ln\left|\frac{|\alpha E+2\lambda|+\sqrt{(\alpha E+2\lambda)^2-4\alpha^2}}{2(t+\sqrt{t^2-\alpha^2})}\right|}. \tag{11}$$

When $|\frac{|\alpha E+2\lambda|+\sqrt{(\alpha E+2\lambda)^2-4\alpha^2}}{2(t+\sqrt{t^2-\alpha^2})}| > 1 (= 1)$, ξ is a finite (infinite) value, and the corresponding state is localized (decolized). Thus, the critical points and MEs are determined by $|\frac{|\alpha E_{2c}+2\lambda|+\sqrt{(\alpha E_{2c}+2\lambda)^2-4\alpha^2}}{2(t+\sqrt{t^2-\alpha^2})}| = 1$, which can give the ME expression [Eq. (4)] (see Appendix B). The ME expression of Model II can also be analytical obtained by using a self-consistent theory [45].

Naturally, combining Eqs. [(9a) and (9b)] and the expression Eq. (4) of Model II's ME, one can obtain the expression Eq. (2) of Model I's ME. From the calculation process, one can see that if the hopping term is exponential, the transfer matrix will become very complicated and the analytical calculation is not technically possible.

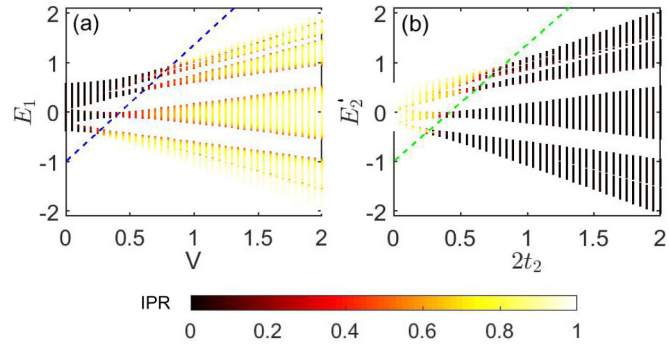

FIG. 1. (a) The IPR of different eigenstates as a function of the corresponding eigenvalues E_1 and quasiperiodic potential strength V with fixed $p = 1.5$ and $t_1 = 1$ in Model I, (b) The IPR as a function of E_2' and $2t_2$ with fixed $\alpha = 0.4251$ and $\lambda = 0.1924$ in Model II. Here the values of α and λ are obtained from Eqs. (9a) and (9b) with fixed $p = 1.5$ and $t_1 = 1$. As Eq. (9b), here $E_2' = E_2 - \frac{2t_1 e^{-2p}}{1+e^{-2p}}$. The blue and green dotted lines in (a) and (b) are obtained from Eq. (2). Here we fix $\beta = (\sqrt{5}-1)/2$ and the size $L = 500$.

C. Numerical results

Now we display the numerical evidence for the dual relation. The numerical results are obtained by calculating the inverse participation ratio (IPR) [3] $\mathrm{IPR}(\kappa) = \sum_{j=1}^{L} |\psi_{\kappa,j}|^4$, where ψ_κ is the κth eigenstate. It is known that tends to zero in the thermodynamic limit for extended states but approaches to a finite value of $O(1)$ for a localized state. Figure 1(a) shows the energy eigenvalues and the IPR of the corresponding eigenstates for Model I as a function of V under OBC. The dotted line represents the ME given in Eq. (2). We see that IPR values are approximately zero for energies above the ME and are finite for energies below the ME. In Fig. 1(a), we take $p = 1.5$ and $t_1 = 1$, which can give $\alpha = 0.4251$ and $\lambda = 0.1924$ from Eqs. (9a) and (9b). Then, fixing t_2, we can diagonalize Model II and obtain its eigenvalues E_2 and the IPR of the corresponding eigenstates. Figure 1(b) shows the IPR as a function of E_2' and $2t_2$, where $E_2' = E_2 - \frac{2t_1 e^{-2p}}{1+e^{-2p}}$ as Eq. (9b). Due to $V = 2t_2$, we take the horizontal axis being $2t_2$ to compare with Fig. 1(a). One can see that the two energy spectrum in Figs. 1(a) and 1(b) are exactly the same, but the IPR values in Fig. 1(b) are finite for energies above the ME and are approximately zero for energies below the ME, which is contrary to Fig. 1(a), indicating that Model I and Model II are mutually dual and their dual relationships satisfy Eqs. (9a) and (9b).

Besides the IPR, we further introduce the Husimi function [49–52] to gain a better intuition for the localization behavior in both the real space and the momentum space. It is given by

$$\rho(j_0, k_0) = |\langle j_0, k_0|\psi\rangle|^2. \tag{12}$$

Here the Husimi function is the probability density function for finding the system with state $|\psi\rangle$ in a

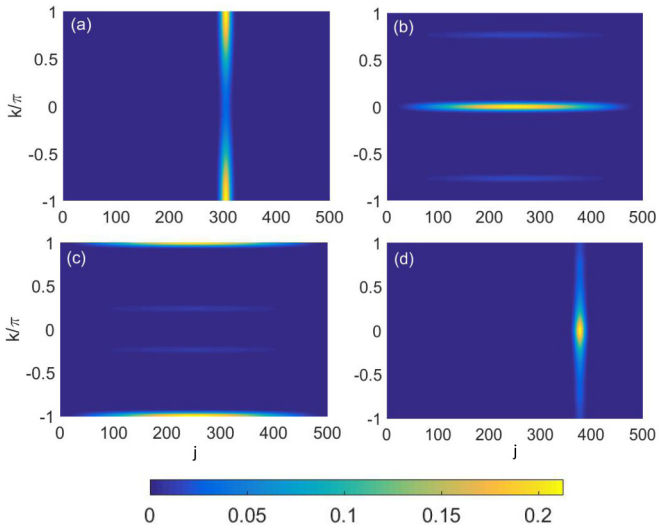

FIG. 2. The Husimi function $\rho(j,k)$ for the eigenstate corresponding the lowest energy in (a) and (c) and highest energy in (b) and (d). (a) and (b) correspond to Model I with $p = 1.5$, $t_1 = 1$, and $V = 0.5$, (c) and (d) correspond to Model II with $\alpha = 0.4251$, $\lambda = 0.1924$, and $t_2 = 0.25$. Here we fix $\beta = (\sqrt{5}-1)/2$ and the size $L = 500$.

minimum-uncertainty state centered at j_0 in coordinate space and at k_0 in momentum space. Note that whereas the momentum is not a good quantum number here, the projection on the selected k_0 can be performed. Using the minimal uncertainty state in real space [51],

$$\langle j|j_0,k_0\rangle = \left(\frac{1}{2\pi\sigma^2}\right)^{1/4} \exp\left[-\frac{(j-j_0)^2}{4\sigma^2} + ik_0(j+j_0/2)\right],$$

where σ is taken as $\sigma = \sqrt{\frac{L}{4\pi}}$ and inserting $\sum_j |j\rangle\langle j|$ in Eq. (12), one can obtain the Husimi function as shown in Fig. 2. From Fig. 2(a), we see that there exists one vertical stripe for the lowest state of Model I indicating that the considered state is localized in real space and extended in momentum space. By contrast, Fig. 2(b) shows three horizontal stripes symmetrically placed with respect to $k = 0$ for the highest state of Model I indicating that the state is localized in momentum space and extended in real space. Comparing Figs. 2(a) with 2(b), we see that there exists a ME for Model I with $p = 1.5$, $t_1 = 1$, and $V = 0.5$, and the eigenstates are spatially localized and extended below and above the ME. The same analysis applies to Model II [see Figs. 2(c) and 2(d)], whose eigenstates are spatially extended and localized below and above the ME, and it is consistent with our conclusion that Model I and Model II are mutually dual.

III. SUMMARY AND DISCUSSION

We have analytically proven that the two widely studied models [Model I (1) and Model II (3)] with exact MEs are mutually dual and obtained their dual relationships. We further numerically verified our result by calculating the IPR and Husimi function. Our conclusion will provide new insights into the ME's study in both theory and experiment. In theory, studying the physical properties of one of the models, one can deduce the corresponding properties of the other model. On the other hand, we provide a new approach to study the system with the exponential hopping, whose some properties are difficult to investigated both numerically and analytically but can be obtained from its dual model. As an example of application, we have analytically obtained the localization length and ME expressions of Model II by using the Avila's global theory and then given Model I's ME expressions by using the dual relation. The ME expressions of the two models are consistent with the previous work [8,9]. In experiment, the realization of Model I and the detection of the location of ME can be replaced by detecting the location of Model II's ME in momentum space, which has been realized and detected recently [44].

ACKNOWLEDGMENTS

Y.W. and X.-J.L. were supported by National Nature Science Foundation of China (Grants No. 11825401, No. 11761161003, and No. 11921005), the National Key R&D Program of China (Grant No. 2016YFA0301604), Guangdong Innovative and Entrepreneurial Research Team Program (Grant No. 2016ZT06D348), the Science, Technology and Innovation Commission of Shenzhen Municipality (Grant No. KYTDPT20181011104202253), the Open Project of Shenzhen Institute of Quantum Science and Engineering (Grant No. SIQSE202003), and the Strategic Priority Research Program of Chinese Academy of Science (Grant No. XDB28000000). X.X. was supported by NanKai Zhide Foundation. Y.W. was supported by the National Natural Science Foudation of China (Grant No. 12061031). Z.Z. acknowledges financial support of the NSF of China (Grants No. 12031020 and No. 11671382), the CAS Key Project of Frontier Sciences (Grant No. QYZDJ-SSW-JSC003), and the Key Laboratory of Random Complex Structures and Data Sciences CAS and National Center for Mathematics and Interdisciplinary Sciences CAS.

APPENDIX A: DUALITY OF AUBRY-ANDRÉ MODEL

In this Appendix, we review the self-duality of the familiar AA model, which is given by

$$Eu_j = t(u_{j+1} + u_{j-1}) + V\cos(2\pi\beta j + \delta)u_j. \tag{A1}$$

For convenience, we set $\delta = 0$. We introduce the Fourier transform of u_j,

$$u_j = \frac{1}{\sqrt{L}}\sum_k u_k e^{-ikj}, \quad u_k = \frac{1}{\sqrt{L}}\sum_j u_j e^{ikj}, \tag{A2}$$

In the momentum space, the AA model can be written as

$$Eu_k = 2t\cos(k)u_k + \frac{V}{2}(u_{k+2\pi\beta} + u_{k-2\pi\beta}). \tag{A3}$$

For a finite-size system, if we take periodic boundary conditions (PBC), we need to approximate the irrational β by $\beta = \frac{M}{L}$ with M and L being coprimes. The momentum can be relabeled by $k = 2n\pi\frac{M}{L} \bmod 2\pi$ with $n = 1, 2, \ldots, L$, then, Eq. (A2) becomes the transformation form [Eq. (5)] in the

main text. We can rewrite Eq. (A3) as

$$E u_n = 2t\ \cos(2\pi\beta n)u_n + \frac{V}{2}(u_{n+1} + u_{n-1}). \tag{A4}$$

where n is the index for the momentum sites with the interval being $2\pi\frac{M}{L}$. Here we show an example of setting β and L in a finite-size system. In most studies β is chosen to be the golden mean, i.e., $\beta = \frac{\sqrt{5}-1}{2}$, which can be approached by $\beta = \lim_{m\to\infty}(F_{m-1}/F_m)$, where the Fibonacci numbers $F_{m+1} = F_{m-1} + F_m$ with $F_0 = F_1 = 1$, taking $M = F_{m-1}$ and the system size $L = F_m$ to ensure the PBC. When taking an OBC in numerical calculations, we can directly take an irrational number β and still use Eq. (A4). Now the interval of the momentum site can be considered as $2\pi\beta$. For a large system, there is no obvious difference between the two, i.e., using the approximation $\beta = \frac{M}{L}$ under the PBC or using the irrational number β under the OBC. In numerical calculations, one needs to consider the boundary conditions and system sizes. However, we do not consider them when making the dual transformation. Thus, one can directly use the transformation form Eq. (5).

APPENDIX B: DETAILS FOR LOCALIZATION LENGTH

In this Appendix, we give the details of the derivation of Lyapunov exponents. For convenience, we set the hopping strength $t_2 = 1$. The transfer matrix (10) can be decomposed into two parts $T^n = A^n B^n$, where

$$A^n = \frac{1}{1 - \alpha\ \cos(2\pi\beta n + \delta)}, \tag{B1}$$

and

$$B^n = \begin{pmatrix} B_{11} & B_{12} \\ B_{21} & 0 \end{pmatrix}, \tag{B2}$$

with $B_{11} = E[1 - \alpha\ \cos(2\pi\beta n + \delta)] - 2\lambda\ \cos(2\pi\beta n + \delta)$ and $B_{21} = -B_{12} = 1 - \alpha\ \cos(2\pi\beta n + \delta)$. Then,

$$\gamma(E) = \gamma_A(E) + \gamma_B(E), \tag{B3}$$

where $\gamma_A = \lim_{n\to\infty}\frac{1}{2\pi L}\int \ln\|A_L(\delta)\|d\delta$ with $A_L = \prod_{n=1}^{L} A^n$. By the ergodic theory, $\gamma_A(E) = \frac{1}{2\pi}\int_0^{2\pi} \ln\left(\frac{1}{1-\alpha\cos(\delta)}\right)d\delta = -\ln\left|\frac{1+\sqrt{1-\alpha^2}}{2}\right|$ [53,54]. In Eq. (B3), $\gamma_B = \lim_{n\to\infty}\frac{1}{2\pi L}\int \ln\|B_L(\delta)\|d\delta$ with $B_L = \prod_{n=1}^{L} B^n$. Below we calculate γ_B relies on Avila's global theory [47]. We first complexify the phase, i.e., $B_{11} = E[1 - \alpha\ \cos(2\pi\beta n + \delta + i\epsilon)] - 2\lambda\ \cos(2\pi\beta n + \delta + i\epsilon)$, $B_{21} = -B_{12} = 1 - \alpha\ \cos(2\pi\beta n + \delta + i\epsilon)$. Then, let ϵ tend to infinity, the matrix B^n becomes

$$B^n(\delta + i\epsilon) = \frac{e^{2\pi\epsilon}e^{i(2\pi\beta n+\delta)}}{2}\begin{pmatrix} -\alpha E - 2\lambda & \alpha \\ -\alpha & 0 \end{pmatrix} + o(1). \tag{B4}$$

Thus, we have $\gamma_B(E,\epsilon) = 2\pi\epsilon + \ln\left|\frac{|\alpha E+2\lambda|+\sqrt{(\alpha E+2\lambda)^2-4\alpha^2}}{4}\right| + o(1)$. By the global theory [47], we obtain $\gamma_B(E) = \ln\left|\frac{|\alpha E+2\lambda|+\sqrt{(\alpha E+2\lambda)^2-4\alpha^2}}{4}\right|$. Plugging $\gamma_A(E)$ and $\gamma_B(E)$ into Eq. (B3), we have $\gamma(E) = \ln\left|\frac{|\alpha E+2\lambda|+\sqrt{(\alpha E+2\lambda)^2-4\alpha^2}}{2(1+\sqrt{1-\alpha^2})}\right|$, which gives the localization length as shown in Eq. (11). As our discussions in the main text, MEs satisfy $\left|\frac{|\alpha E+2\lambda|+\sqrt{(\alpha E+2\lambda)^2-4\alpha^2}}{2(1+\sqrt{1-\alpha^2})}\right| = 1$. Now we set $P = \alpha E + 2\lambda$, then, MEs satisfy $|P| + \sqrt{P^2 - 4\alpha^2} = 2(1 + \sqrt{1-\alpha^2})$, which gives $|P| = 2$, i.e., $|\alpha E + 2\lambda| = 2$, which can give Eq. (4) in the main text.

[1] P. W. Anderson, Absence of diffusion incertain random lattices, Phys. Rev. **109**, 1492 (1958).

[2] A. Lagendijk, B. Tiggelen, and D. S. Wiersma, Fifty years of Anderson localization, Phys. Today **62**(8), 24 (2009).

[3] F. Evers and A. D. Mirlin, Anderson transitions, Rev. Mod. Phys. **80**, 1355 (2008).

[4] R. Whitney, Most Efficient Quantum Thermoelectric at Finite Power Output, Phys. Rev. Lett. **112**, 130601 (2014).

[5] C. Chiaracane, M. T. Mitchison, A. Purkayastha, G. Haack, and J. Goold, Quasiperiodic quantum heat engines with a mobility edge, Phys. Rev. Res. **2**, 013093 (2020).

[6] K. Yamamoto, A. Aharony, O. Entin-Wohlman, and N. Hatano, Thermoelectricity near Anderson localization transitions, Phys. Rev. B **96**, 155201 (2017).

[7] E. Abrahams, P. W. Anderson, D. C. Licciardello, and T. V. Ramakrishnan, Scaling Theory of Localization: Absence of Quantum Diffusion in Two Dimensions, Phys. Rev. Lett. **42**, 673 (1979).

[8] J. Biddle and S. Das Sarma, Predicted Mobility Edges in One-Dimensional Incommensurate Optical Lattices: An Exactly Solvable Model of Anderson Localization, Phys. Rev. Lett. **104**, 070601 (2010).

[9] S. Ganeshan, J. H. Pixley, and S. Das Sarma, Nearest Neighbor Tight Binding Models with An Exact Mobility Edge in One Dimension, Phys. Rev. Lett. **114**, 146601 (2015).

[10] Y. Wang, X. Xia, L. Zhang, H. Yao, S. Chen, J. You, Q. Zhou, and X.-J. Liu, One Dimensional Quasiperiodic Mosaic Lattice with Exact Mobility Edges, Phys. Rev. Lett. **125**, 196604 (2020).

[11] J. Biddle, D. J. Priour, Jr., B. Wang, and S. Das Sarma, Localization in one-dimensional lattices with non-neighbor hopping: Generalized Anderson and Aubry-Andre models, Phys. Rev. B **83**, 075105 (2011).

[12] X. Li, and S. Das Sarma, Mobility edges and intermediate phase in one-dimensional incommensurate lattice potentials, Phys. Rev. B **101**, 064203 (2020).

[13] Y. Wang, C. Cheng, X.-J. Liu, and D. Yu, Many-Body Critical Phase: Extended and Nonthermal, Phys. Rev. Lett. **126**, 080602 (2021).

[14] Y. Wang, L. Zhang, S. Niu, D. Yu, and X.-J. Liu, Realization and detection of non-ergodic critical phases in optical Raman lattice, Phys. Rev. Lett. **125**, 073204 (2020).

[15] T. Xiao, D. Xie, Z. Dong, T. Chen, W. Yi, and B. Yan, Observation of topological phase with critical localization in quasi-periodic lattice, arXiv:2011.03666.

[16] S. Aubry and G. André, Analyticity breaking and Anderson localization in incommensurate lattices, Ann. Israel Phys. Soc. **3**, 133 (1980).

[17] G. Roati, C. D'Errico, L. Fallani, M. Fattori, C. Fort, M. Zaccanti, G. Modugno, M. Modugno, and M. Inguscio, Anderson localization of a non-interacting Bose-Einstein condensate, Nature (London) **453**, 895 (2008).

[18] S. Iyer, V. Oganesyan, G. Refael, and D. A. Huse, Many-body localization in a quasiperiodic system, Phys. Rev. B **87**, 134202 (2013).

[19] Y. Wang, H. Hu, and S. Chen, Many-body ground state localization and coexistence of localization and extended states in an interacting quasiperiodic system, Eur. Phys. J. B **89**, 77 (2016).

[20] S. Xu, X. Li, Y.-T. Hsu, B. Swingle, and S. Das Sarma, Butterfly effect in interacting Aubry-Andre model: thermalization, slow scrambling, and many-body localization, Phys. Rev. Res. **1**, 032039(R) (2019).

[21] M. Schreiber, S. S. Hodgman, P. Bordia, H. P. Lüschen, M. H. Fischer, R. Vosk, E. Altman, U. Schneider, and I. Bloch, Observation of many-body localization of interacting fermions in a quasirandom optical lattice, Science **349**, 842 (2015).

[22] H. P. Lüschen, P. Bordia, S. Scherg, F. Alet, E. Altman, U. Schneider, and I. Bloch, Observation of Slow Dynamics Near the Many-Body Localization Transition in One-Dimensional Quasiperiodic Systems, Phys. Rev. Lett. **119**, 260401 (2017).

[23] X. Deng, S. Ray, S. Sinha, G. V. Shlyapnikov, and L. Santos, One-Dimensional Quasicrystals with Power-Law Hopping, Phys. Rev. Lett. **123**, 025301 (2019).

[24] S. Das Sarma, S. He, and X. C. Xie, Mobility Edge in a Model One-Dimensional Potential, Phys. Rev. Lett. **61**, 2144 (1988).

[25] J. Biddle, B. Wang, D. J. Priour, Jr., and S. Das Sarma, Localization in one-dimensional incommensurate lattices beyond the Aubry-André model, Phys. Rev. A **80**, 021603(R) (2009).

[26] X. Li, X. Li, and S. Das Sarma, Mobility edges in one dimensional bichromatic incommensurate potentials, Phys. Rev. B **96**, 085119 (2017).

[27] L. Zhou, H. Pu, and W. Zhang, Anderson localization of cold atomic gases with effective spin-orbit interaction in a quasiperiodic optical lattice, Phys. Rev. A **87**, 023625 (2013).

[28] M. Kohmoto and D. Tobe, Localization problem in a quasiperiodic system with spin-orbit interaction, Phys. Rev. B **77**, 134204 (2008).

[29] H. Yao, H. Khoudli, L. Bresque, and L. Sanchez-Palencia, Critical Behavior and Fractality in Shallow One-Dimensional Quasiperiodic Potentials, Phys. Rev. Lett. **123**, 070405 (2019).

[30] Z. Xu, H. Huangfu, Y. Zhang, and S. Chen, Dynamical observation of mobility edges in one-dimensional incommensurate optical lattices, New. J. Phys. **22**, 013036 (2020).

[31] X. Li, S. Ganeshan, J. H. Pixley, and S. Das Sarma, Many Body Localization and Quantum Non-Ergodicity in a Model with a Single-Particle Mobility Edge, Phys. Rev. Lett. **115**, 186601 (2015).

[32] R. Modak and S. Mukerjee, Many Body Localization in the Presence of a Single Particle Mobility Edge, Phys. Rev. Lett. **115**, 230401 (2015).

[33] X. Li, J. H. Pixley, D.-L. Deng, S. Ganeshan, and S. Das Sarma, Quantum nonergodicity and fermion localization in a system with a single-particle mobility edge, Phys. Rev. B **93**, 184204 (2016).

[34] X. B. Wei, C. Cheng, G. Xianlong, and R. Mondaini, Investigating many-body mobility edges in isolated quantum systems, Phys. Rev. B **99**, 165137 (2019).

[35] Y. Liu, X.-P. Jiang, J. Cao, and S. Chen, Non-Hermitian mobility edges in one-dimensional quasicrystals with parity-time symmetry, Phys. Rev. B **101**, 174205 (2020).

[36] Q.-B. Zeng and Y. Xu, Winding numbers and generalized mobility edges in non-Hermitian systems, Phys. Rev. Res. **2**, 033052 (2020).

[37] T. Liu, H. Guo, Y. Pu, and S. Longhi, Generalized Aubry-Andre self-duality and mobility edges in non- Hermitian quasiperiodic lattices, Phys. Rev. B **102**, 024205 (2020).

[38] F. Jendrzejewski, A. Bernard, K. Mueller, P. Cheinet, V. Josse, M. Piraud, L. Pezzé, L. Sanchez-Palencia, A. Aspect, and P. Bouyer, Three-dimensional localization of ultracold atoms in an potical disordered potential, Nat. Phys. **8**, 398 (2012).

[39] W. McGehee, S. Kondov, W. Xu, J. Zirbel, and B. DeMarco, Three-Dimensional Anderson Localization in Variable Scale Disorder, Phys. Rev. Lett. **111**, 145303 (2013).

[40] G. Semeghini, M. Landini, P. Castilho, S. Roy, G. Spagnolli, A. Trenkwalder, M. Fattori, M. Inguscio, and G. Modugno, Measurement of the mobility edge for 3D Anderson localization, Nat. Phys. **11**, 554 (2015).

[41] H. P. Lüschen, S. Scherg, T. Kohlert, M. Schreiber, P. Bordia, X. Li, S. D. Sarma, and I. Bloch, Single-Particle Mobility Edge in a One-Dimensional Quasiperiodic Optical Lattice, Phys. Rev. Lett. **120**, 160404 (2018).

[42] F. A. An, E. J. Meier, and B. Gadway, Engineering a Flux-Dependent Mobility Edge in Disordered Zigzag Chains, Phys. Rev. X **8**, 031045 (2018).

[43] T. Kohlert, S. Scherg, X. Li, H. P. Lüschen, S. D. Sarma, I. Bloch, and M. Aidelsburger, Observation of Many-Body Localization in a One-Dimensional System with Singleparticle Mobility Edge, Phys. Rev. Lett. **122**, 170403 (2019).

[44] F. A. An, K. Padavic, E. J. Meier, S. Hegde, S. Ganeshan, J. H. Pixley, S. Vishveshwara, and B. Gadway, Observation of Tunable Mobility Edges in Generalized Aubry-André Lattices, Phys. Rev. Lett. **126**, 040603 (2021).

[45] A. Duthie, S. Roy, and D. E. Logan, Self-consistent theory of mobility edges in quasiperidic chains, Phys. Rev. B **103**, L060201 (2021).

[46] Y. Zhang, A. V. Maharaj, and S. A. Kivelson, Are there quantum oscillations in an incommensurate charge density wave?, Phys. Rev. B **91**, 085105 (2015).

[47] A. Avila, Global theory of one-frequency Schrödinger operators, Acta. Math. **1**, 215 (2015).

[48] X. Xia, Y. Wang, J. You, Z. Zheng, and Q. Zhou, Exact mobility edges for 1D quasicrystals (unpublished).

[49] K. Husimi, Some formal properties of the density matrix, Proc. Phys. Math. Soc. Jpn. **22**, 264 (1940).

[50] J. E. Harriman, Some properties of the Husimi function, J. Chem. Phys. **88**, 6399 (1988).

[51] C. Aulbach, A. Wobst, G.-L. Ingold, P. Hänggi, and I. Varga, Phase-space visualization of a metal-insulator transition, New J. Phys. **6**, 70 (2004).

[52] J. Feist, A. Bcker, R. Ketzmerick, S. Rotter, B. Huckestein, and J. Burgdrfer, Nanowires with Surface Disorder: Giant Localization Lengths and Quantum-to-Classical Crossover, Phys. Rev. Lett. **97**, 116804 (2006).

[53] I. S. Gradshteyn and I. M. Ryzhik, *Table of Integrals, Series, and Products*, 6th ed. (Academic, New York, 2000).

[54] S. Longhi, Metal-insulator phase transition in a non-Hermitian Aubry-André-Harper model, Phys. Rev. B **100**, 125157 (2019).